

Assessment and characterisation of common renal masses with CT and MRI

Leo Pallwein-Prettner · Daniel Flöry · Claus Raphael Rotter · Kurt Pogner ·
Gerhard Syré · Claudia Fellner · Ferdinand Frauscher · Friedrich Aigner ·
Frens Steffen Krause · Franz Fellner

Received: 18 November 2010 / Revised: 12 May 2011 / Accepted: 28 June 2011 / Published online: 17 July 2011
© European Society of Radiology 2011

Abstract

Objective Owing to the widespread use of abdominal imaging studies the detection rate of solid renal masses has increased, and an accurate characterisation of imaging features of renal masses has become more essential for case management.

Method and results MR imaging (MRI) and computed tomography (CT) are frequently used modalities for detection and differentiation of renal masses. This article gives a review of imaging characteristics of benign and malignant renal masses, discussing their appearance in CT and MR imaging. Advanced MR techniques like diffusion-weighted imaging and apparent diffusion coefficient (ADC) mapping, which have shown promising results in the differentiation between benign and malignant renal lesions, will be introduced.

Conclusion MRI and CT are useful in the characterisation and estimation of the prognosis for renal masses.

Keywords Humans · Kidney diseases · Kidney masses · Magnetic resonance imaging · Computed tomography

Introduction/epidemiology

The detection rate of renal masses has increased in the last decades owing to the widespread use of CT and MRI [1]. Therefore, an accurate characterisation of renal masses is essential to ensure appropriate case management. Renal masses can be divided into cystic and solid lesions [2]. The most common are cysts in up to 27% of patients over 50 years [3]. CT- or MRI-enhancing masses are classified as solid or complex cystic. Eighty-five percent of expansive solid masses are malignant [4]. Therefore, a solid, enhancing mass must be considered malignant unless proven otherwise. Renal cell carcinoma (RCC) is the most common malignant tumour with a rising incidence of about 3% per year since 1975. The most common subtype of RCC is the clear cell RCC (synonym: common or conventional RCC) with 65% of renal cortical tumours. Further subtypes are papillary (basophilic and eosinophilic) and chromophobe RCCs with about 25% of renal cortical tumours. Clear-cell RCC causes 90% of metastases of all renal malignancies [5, 6]. Other malignant masses include transitional cell carcinoma (TCC), lymphoma (primary and more frequent secondary), metastases from carcinoma and primary/secondary sarcoma. Primary tumours of the lung, breast and gastrointestinal tract are the most common sources of renal metastases [7].

Benign tumours account for approximately 20% of all solid renal cortical tumours, and renal oncocytoma is the most common solid tumour type [8, 9].

Non-neoplastic renal masses include inflammatory pseudotumours with and without abscess formation, renal

L. Pallwein-Prettner (✉) · D. Flöry · F. Fellner
Department of Radiology, General Hospital Linz,
Krankenhausstrasse 9,
4020 Linz, Austria
e-mail: leo.pallwein-prettnr@bhs.at

C. R. Rotter · K. Pogner · F. S. Krause
Department of Urology, General Hospital Linz,
Linz, Austria

G. Syré
Department of Pathology, General Hospital Linz,
Linz, Austria

C. Fellner
Institute of Radiology, University Medical Center Regensburg,
Regensburg, Germany

F. Frauscher · F. Aigner
Department of Radiology, Medical University Innsbruck,
Innsbruck, Austria

infarct, haematoma and replacement lipomatosis with coexistent xanthogranulomatous pyelonephritis [10, 11].

Examination protocol

The examination protocols of CT and MR are abundantly described elsewhere and we refer to the current literature [12–15].

CT A renal CT is performed in 3–4 phases: the native, arterial (20- to 40-s delay), the venous (100- to 150-s delay) and the excretory phase (180- to 300-s delay). In order to reduce radiation exposure, different low-dose protocols and a reduction of contrast phases have been reported [14].

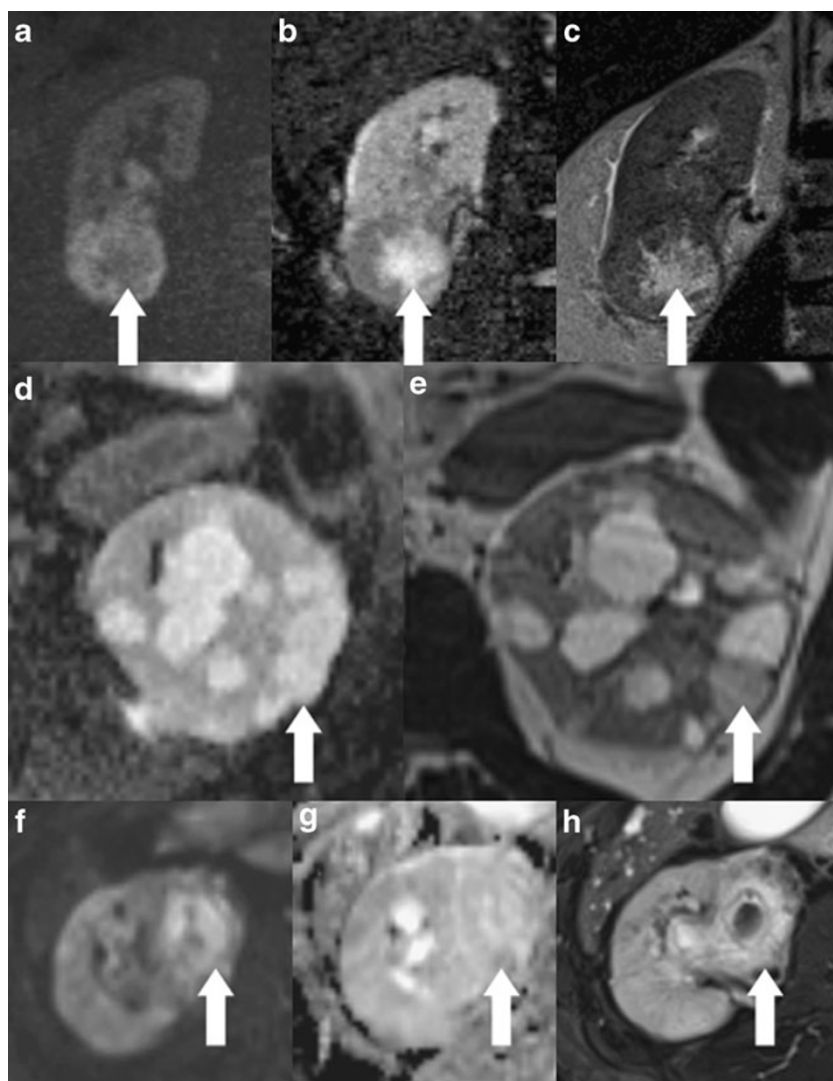
MRI MR examinations are performed with dedicated body (array) coils and must include T1-weighted gradient-echo (GRE, in- and opposed-phase) and T2-weighted turbo spin

echo (TSE) sequences. Dynamic gadolinium-enhanced images are obtained in late arterial (20-s delay), nephrographic (80-s delay) and excretory phases (180-s delay). As in CT, MR urograms can be obtained ideally with thick-slab single-shot T2-weighted TSE.

The use of furosemide for forced diuresis and a further distension of the collecting system and for a consecutive reduction in the T2* effects of the concentrated contrast material is optional [13, 15].

Concerning diffusion-weighted imaging (DWI) [16], different authors have shown the value of apparent diffusion coefficients (ADCs) for characterising renal masses. In these studies, renal tumours had significantly lower ADCs compared with benign cysts, and solid enhancing tumours had significantly lower ADCs compared with non-enhancing necrotic or cystic regions [17, 18]. They concluded that ADC measurements may aid in differentiating subgroups of renal masses, particularly benign cystic lesions from cystic renal cell cancers (Fig. 1).

Fig. 1 Presentation of diffusion-weighted images (DWI; b-value: 800) and apparent diffusion coefficient (ADC) maps in different entities: Upper row demonstrates bright signal on DWI (a; b-value: 800) and low signal on an ADC map (b) in the case of a clear cell renal cell carcinoma (RCC), with heterogeneous pattern on T2-weighted image (c). The signal decrease in the ADC map is considered to be a marker of high cell density in the tumour. Middle row demonstrates bright signal on the ADC map (d) in a polycystic kidney. T2-weighted image shows different intensities in the cysts (arrow in e). The cysts were graded as Bosniak I–II. Lower row demonstrates bright signal on DWI (f; b-value: 800) in a case of xanthogranulomatous pyelonephritis (see also Fig. 10). The ADC map (g) showed no signal loss, which could be explained by interstitial oedema but no indication of increased cell density, which can be helpful in the differentiation of an inflammatory from a neoplastic tissue alteration. Contrast-enhanced T1-weighted image shows strong enhancement of the pelvic wall (arrow in h)



Imaging parameters of renal masses

These imaging parameters should be helpful in the characterisation of renal masses focussing especially on differentiation between cystic and solid lesions [19].

- I. Detection of lesions: Because of better soft-tissue contrast the tumour detection rate seems better with MR, but according to the literature, especially in renal lesions with a diameter of more than 2 cm, CT shows a similar detection rate [20].
- II. Size, shape and contour: Renal masses with a diameter of <4 cm are defined as small renal masses. The smaller the mass is, the greater the chance that it is benign [1]. In a report 46% of masses that were less than 1 cm in diameter were benign, as were 22% of those that were 1 to 2.9 cm in diameter and 20% of those that were 3 to 3.9 cm in diameter [21]. Among malignant masses, greater size correlates with higher pathological grade [4, 22–24]. As in many other malignancies, unsharpened borders of a solid tumour are nearly always a sign of malignancy with the exception of inflammatory cysts and bleeding angiomyolipoma.
- III. Growth rate: Growth rate of small renal masses is typically low (2 to 4 mm per year) and seems to be similar for masses subsequently found to be malignant (renal cell carcinoma) and those found to be benign (oncocytoma) [26]. Masses without growth were about as likely to be malignant (83%) as those that grew (89%) [27]. There are no definable clinical or radiological characteristics to predict growth [22].
- IV. Tissue consistency: Areas of macroscopic fat within a renal mass are usually diagnostic of angiomyolipoma with a very few exceptions. In rare cases the additional presence of calcification in a fat-containing lesion can indicate a malignant condition [28, 29]. A small number of angiomyolipomas do not contain fat and remain a diagnostic dilemma because differentiation from malignant renal neoplasm is impossible [30]. On the other hand, a few cases of RCC have been reported where macroscopic fat and calcifications were present [31].

Presence of central necrosis may be helpful in the diagnosis of RCC, a finding that is very rare in angiomyolipoma [32]. Intratumoral haemorrhage has a variable appearance depending on the stage of degradation of the component blood products. Subacute to chronic haemorrhage generally demonstrates high signal intensity on both T1- and T2-weighted images. Chronic haemorrhage, containing haemosiderin, is typically hypointense on both T1- and T2-weighted images [33]. Intratumoral bleeding is sometimes hard to depict with CT, while calcifications can hardly be seen on MRI.

V. Imaging characteristics of common renal masses

The imaging characteristics of common renal masses are listed in Table 1.

1. Simple/Complex cyst:

The Bosniak classification system is used to graduate cystic masses: [34]

- Bosniak I: Benign simple cyst, hairline-thin wall, no septa, calcifications or solid components. Water density, no contrast enhancement.
- Bosniak II: Benign cyst, may contain few hairline-thin septa. Fine calcification or slightly thickened calcification in wall or septa. Uniformly high-attenuation lesions (<3 cm), sharply marginated, no enhancement, are included in this group.
- Bosniak IIF: Increased number of hairline-thin septa. Minimal enhancement in hairline-thin smooth septum or wall, minimal thickening of the septa or wall. Possibly thick and nodular calcification, no contrast enhancement. No enhancing soft-tissue components. Totally intrarenal nonenhancing high-attenuation renal lesions that are 3 cm or larger are also included in this category. These lesions are generally well marginated.
- Bosniak III: Indeterminate cystic masses with thickened irregular walls or septa, enhancement can be seen.
- Bosniak IV: Clearly malignant cystic masses, additionally with enhancing soft-tissue components adjacent to but independent of the wall or septa.

CT It is helpful to differentiate category I, III and IV cysts. Depending on the size and location, it is critical to differentiate between complicated cysts of categories II and III [35].

The so-called pseudoenhancement is defined as an artificial elevation of the Hounsfield unit measurements of a renal cyst measured on the contrast-enhanced CT images and is thought to be secondary to the image reconstruction algorithm used to adjust for beam-hardening effects. This pseudoenhancement of small intraparenchymal cysts can lead to an upgraded Bosniak cyst classification with major implications for prognosis and clinical management. Also, calcification and high-density fluid of cysts can complicate the differentiation between Bosniak II and III cysts [2, 31].

MRI Simple cysts are homogeneous hyperintense lesions with a thin wall on T2-weighted images (Fig. 2). Complex cysts have septa and solid nodules with low signal on T2-weighted images due to haemorrhagic or proteinaceous content (Fig. 3). On T1-weighted images simple cysts are hypointense relative to the normal renal parenchyma.

Table 1 CT and MRI imaging characteristics of common renal masses

Renal mass	CT [12–14, 20, 25, 31, 39, 43]	MRI [32–34, 40, 43, 47, 50, 52]	Enhancement pattern #	T1 (#)	T2 (#)	Enhancement pattern (#)
Simple cyst	No enhancement	Hypointense	No enhancement	Hypointense	Hyperintense	No enhancement
Complex cyst	Mural/septal (nodular) enhancement	Hypo-, hyperintense (depends on haemorrhage or proteinaceous fluid)	Mural/septal (nodular) enhancement	Hypo-, hyperintense (depends on haemorrhage or proteinaceous fluid)	Hypo-, hyperintense (depends on haemorrhage or proteinaceous fluid)	Mural/septal (nodular) enhancement
RCC clear cell	Hyperenhancement (90%); heterogeneous pattern (90%) (cystic/necrotic)	Isointense (cytoplasmatic fat; in-, opp phase); hypointense in case of necrosis	Hyperenhancement (90%); heterogeneous pattern (90%) (cystic/necrotic)	Isointense (cytoplasmatic fat; in-, opp phase); hypointense in case of necrosis	Hyperintense (hypointense in case of haemorrhage)	Hyperenhancement (90%); heterogeneous pattern (90%) (cystic/necrotic)
RCC papillary	Hypoenhancement (57%); homogeneous pattern (90%)	Isointense	Hypoenhancement (57%); homogeneous pattern (90%)	Isointense	Hypointense	Hypoenhancement; homogeneous pattern (heterogeneous in case of necrosis)
TCC	Hypoenhancement; heterogeneous pattern	Isointense (to medulla)	Hypoenhancement; heterogeneous pattern	Isointense (to medulla)	Hypointense (in the case of infiltration)	Hypoenhancement; filling defects in the collecting system
Lymphoma	Hypoenhancement; heterogeneous pattern	Iso-hypointense	Hypoenhancement; heterogeneous pattern	Iso-hypointense	Hypointense	Hypoenhancement; heterogeneous pattern
Adenoma/oncocytoma	Hyper-, hypo-enhancement; heterogeneous pattern; central scar	Hypointense (70%)	Hyper-, hypo-enhancement; heterogeneous pattern; central scar	Hypointense (70%)	Hyperintense (67%)	Hyper-, hypo-enhancement; heterogeneous pattern; central scar
Abscess/Mural enhancement; heterogeneous pattern	xantho/granuloma. PN (hydronephrosis)	Mural enhancement; heterogeneous pattern (calculi, hydronephrosis)	xantho/granuloma. PN (hydronephrosis)	Mural enhancement; heterogeneous pattern (calculi, hydronephrosis)	Isointense	Hyperintense
Angiomyolipoma	Hypo-, hyperenhancement; fat-containing	Hyperintense; bulk fat (fat saturation)	Hypo-, hyperenhancement; fat-containing	Hyperintense; bulk fat (fat saturation)	Hyperintense; (hypointense in lipid-poor AML)	hypo-, hyperenhancement
Pseudotumour	Enhancement equal to normal tissue	Isointense	Enhancement equal to normal tissue	Isointense	Isointense	Enhancement equal to normal tissue

#Density/intensity compared with renal parenchyma

Fig. 2 MRI presentation of typical image characteristics of a simple cyst (Bosniak I): hyperintense on T2-weighted images (T2; arrow in **a**), hypointense on T1-weighted images (T1; arrow in **b**), no contrast media enhancement in T1 (arrow in **c**), and bright on the diffusion-weighted images (ADC map; arrow in **d**)

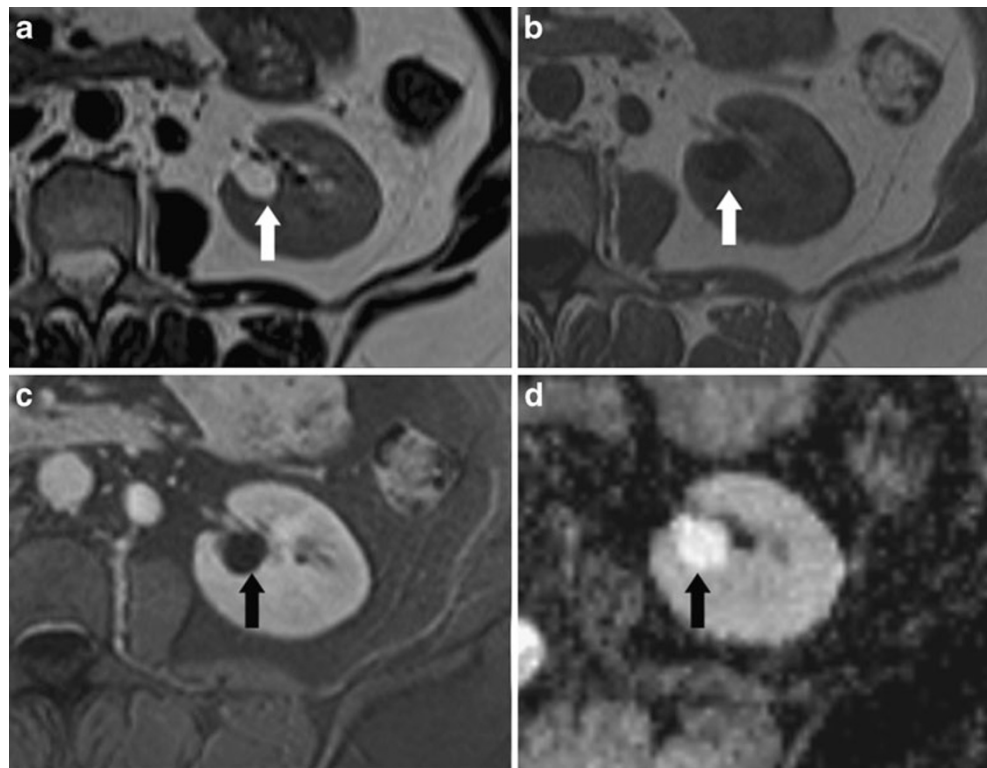
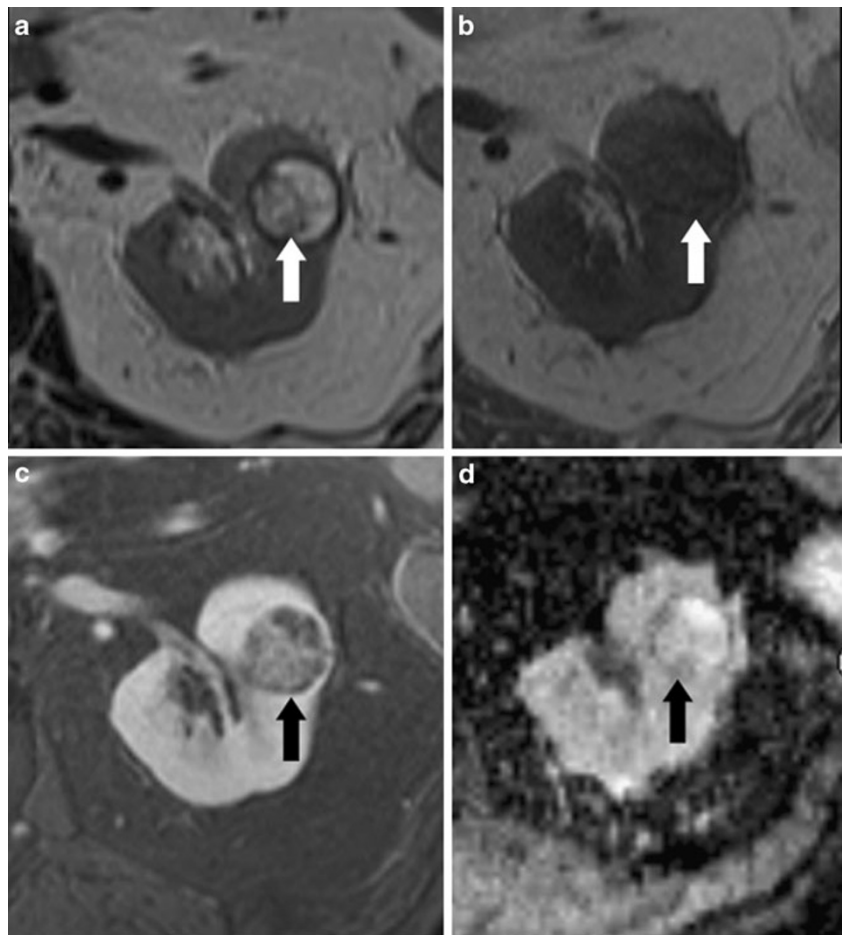


Fig. 3 MRI presentation of typical image characteristics of a complex cyst (Bosniak IV): hyperintense with hypointense areas on T2- (arrow in **a**), hypo- and isointense in T1- (arrow in **b**), focal contrast media enhancement on T1-weighted (arrow in **c**), and heterogeneous pattern on the ADC map (arrow in **d**)



Increased signal may indicate haemorrhage or proteinaceous fluid [32].

Israel et al. compared CT and MRI in the evaluation of cystic renal masses by using the Bosniak classification system. CT and MRI findings were similar for most cystic renal masses. In some cases, however, MRI may depict additional septa, thickening of the wall and/or septa, or enhancement, which may lead to an upgraded Bosniak classification [34]. Nevertheless, it is helpful to be aware that the Bosniak criteria have been defined and validated for CT and not for MRI. Therefore, the Bosniak criteria have to be used carefully used in relation to magnetic resonance imaging.

Despite the use of contrast-enhanced ultrasound (CEUS) in the differential diagnosis of renal masses still being under debate, complex cysts of the kidney are probably the best indication for renal CEUS. CEUS helps to depict blood flow perfusion within the wall, septa and solid components. Furthermore, CEUS is applicable in patients with impaired kidney function or ureteric obstruction, which may be contraindications for contrast-enhanced CT or MRI [36].

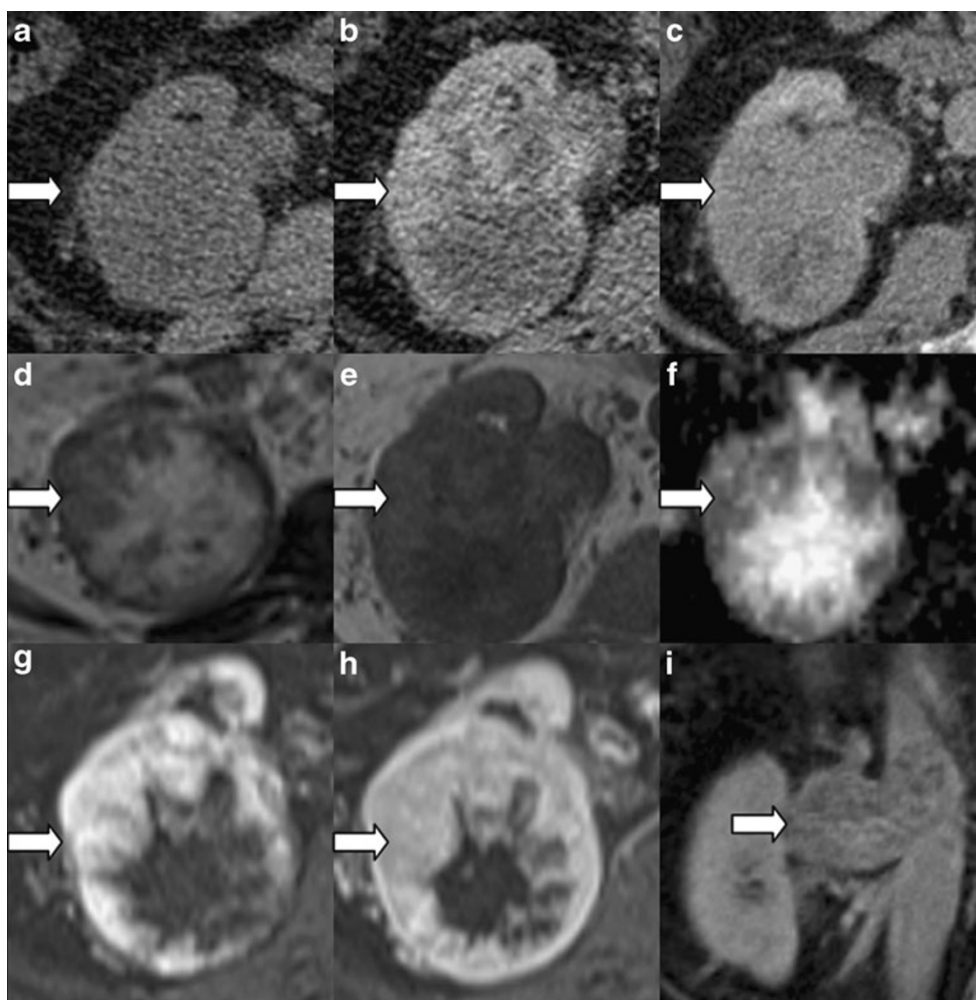
2. RCC (clear cell or common type)

The Fuhrman grading system categorises clear cell carcinoma into four groups (Fig. 4). Its use has been expanded to other subtypes (e.g., papillary RCC). The following tumours have a poorer prognosis: high-grade carcinoma, clear cell RCC, sarcomatoid and rhabdoid differentiations of clear cell RCC [37, 38].

CT Ninety percent of clear cell RCCs are hypervascular with a heterogeneous enhancing pattern of mixed enhancing solid soft-tissue components and low-attenuation necrotic or cystic areas [13, 39]. Clear cell carcinomas can be predominantly cystic. Renal vein tumour thrombus can be seen with aggressive higher stage tumours.

MRI Appearance varies depending on the presence of haemorrhage and necrosis. On T1-weighted images clear cell RCC most frequently demonstrates a signal intensity as renal parenchyma. Central necrosis is typically seen as a homogeneous hypointense area in the centre of the mass on

Fig. 4 Multimodal presentation of a common type RCC on CT and MRI: CT (upper row): isodense in the native phase (arrow in **a**), hypervascular in the arterial phase with areas of necrosis (arrow in **b**) and early wash-out in the venous phase (arrow in **c**). MRI (middle and lower row): heterogeneous appearance on T2-weighted (arrow in **d**) and T1-weighted native (arrow in **e**) because of haemorrhage and necrosis, heterogeneous pattern on the ADC map (arrow in **f**), hyper-enhancement in the arterial phase with areas of necrosis (arrow in **g**), early wash-out in the venous phase (arrow in **h**), and a tumour thrombus with contrast media enhancement reaching the renal vein and inferior vena cava (arrow in **i**)



T1-weighted images. On T2-weighted images an increased signal intensity is found. Loss of signal within the solid portions of the clear cell RCCs on opposed-phase images compared with in-phase images is due to cytoplasmic fat and has been observed in up to 60% of these tumours [30, 32]. Clear cell RCC tends to be hypervascular, with heterogeneous enhancement during the arterial phase [32].

3. RCC (papillary and chromophobe type)

Papillary RCC accounts for approximately 10%–15% of all RCCs and may be multifocal (Fig. 5). Chromophobe renal tumours account for approximately 4–11% of RCCs [32].

CT Seventy-five percent of papillary RCCs are hypovascular, and 90% of all papillary tumours demonstrate a homogeneous or peripheral enhancement pattern. Chromophobe tumours often demonstrate a moderate degree of enhancement [13, 39].

MRI Papillary RCC demonstrates homogeneous low signal intensity on T2-weighted images with homogeneous low-level enhancement after i.v. gadolinium administration. Chromophobe RCC may show cystic changes within a solid tumour. Central necrosis may be absent even in very large chromophobe carcinomas. Imaging features can be identical to those of clear cell RCC [32, 40, 41].

4. TCC

Transitional cell carcinoma (Fig. 6) accounts for 90% of all tumours arising from the renal pelvic urothelium and is divided into papillary (more common) and non-papillary types. TCC is frequently multifocal and may involve any part of the collecting system. Haematogenous spread is less common than with RCC, but lymphatic metastases occur

early. Only 2–4% of patients with bladder cancer develop upper tract TCC, but 40% of patients with upper tract TCC develop bladder cancer. Diagnosis of upper tract TCC is heavily dependent on imaging. Stage is the main predictor of prognosis in comparison to tumour grade [32, 42].

CT CT urography allows assessment of a non-functioning kidney that is superior to excretion urography and nodal and distant metastases. The shape of the kidney is usually preserved even in the presence of large tumours. Hydro-nephrosis proximal to the lesion is usually present unless the collecting system is completely filled by tumour. If the renal sinus is obliterated by tumour, the appearance may mimic the so-called faceless kidney [44].

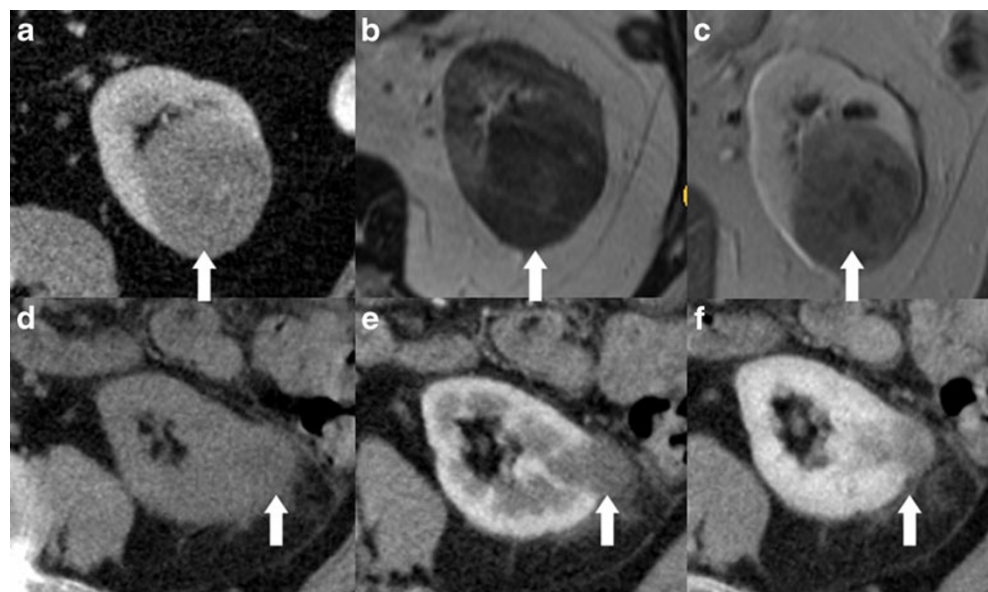
MRI On T1-weighted images TCCs are typically isointense relative to the renal medulla. Enhancement of a focal filling defect in the collecting system is strongly suggestive of a TCC. Differentiation between blood clots and enhancing filling defects may be possible using subtracted data sets. TCC is typically a hypo-enhancing mass, although focal hyper-enhancement may occur.

T2-weighted images show hypointense filling defects in the collecting system. Infiltrative TCC can be seen on single-shot T2-weighted images as a hypointense soft-tissue mass infiltrating the renal parenchyma.

5. Lymphoma

Extranodal spread of lymphoma (Fig. 7) often affects the genitourinary system, with the kidneys being the most commonly involved organs. Primary renal lymphoma is rare, and non-Hodgkin's lymphoma is much more common than Hodgkin's. Growth of lymphomatous cells occurs in

Fig. 5 Imaging presentation of a papillary (upper row) and a chromophobe (lower row) RCC. Papillary RCC (**a**: CT venous phase; **b**: T2-weighted; **c**: T1-weighted, venous phase) as well as chromophobe RCC (**d**: CT native; **e**: CT, arterial phase; **f**: CT, venous phase) show a hypoenhancement in the arterial (arrow in **e**) and venous phase (arrows in **a**, **c** and **f**), and they are often hypo-/isointense on T2-w (arrow in **b**) in comparison to normal renal parenchyma



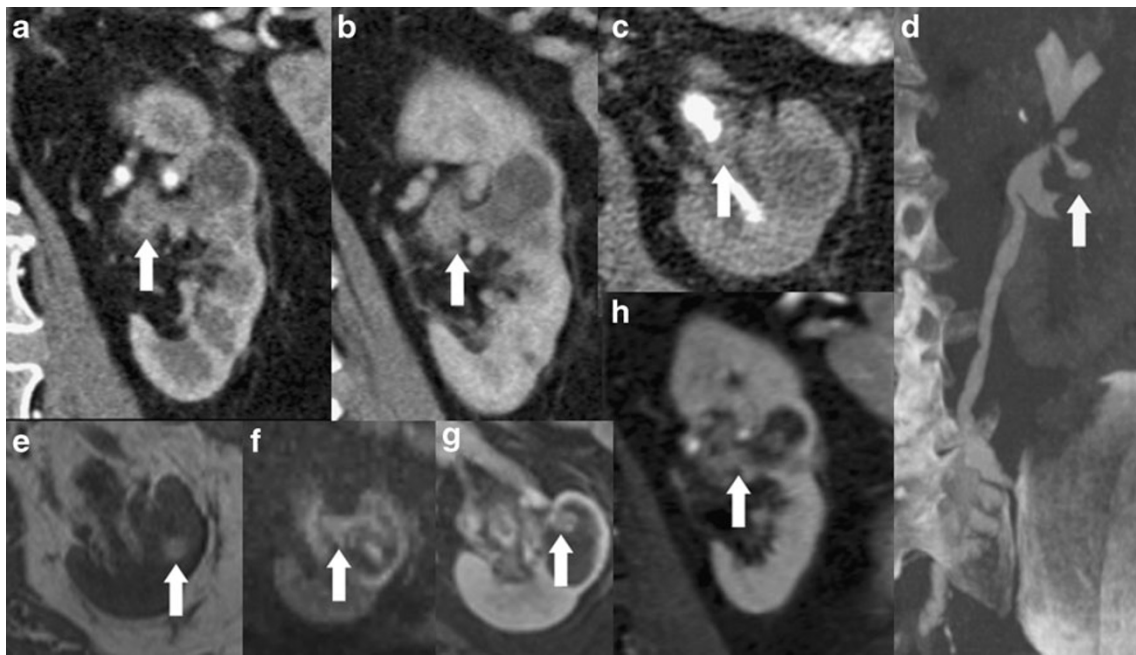


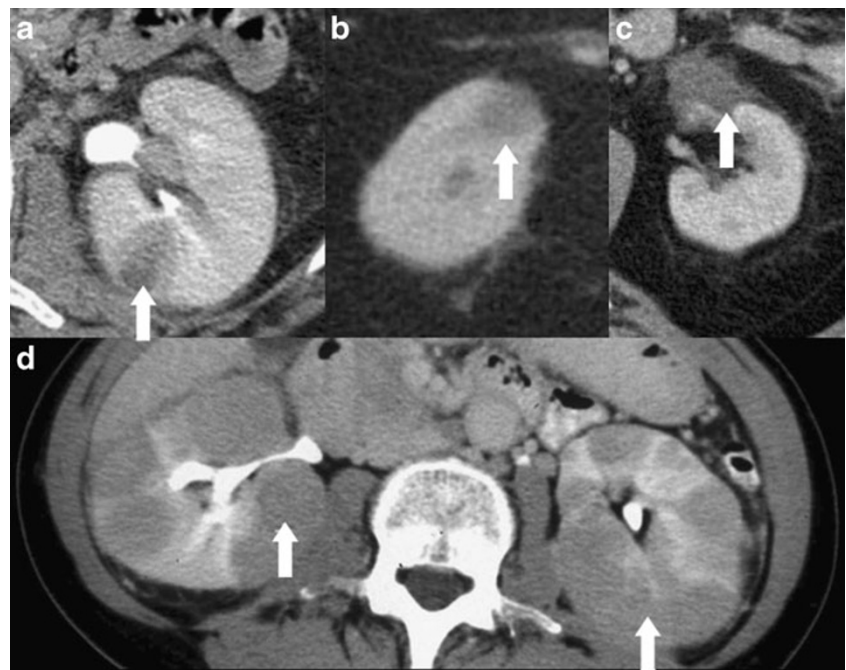
Fig. 6 Imaging presentation of an infiltrating papillary transitional cell carcinoma (TCC) on CT (upper row; **a–d**) and MRI (lower row; **e–h**). On CT there is an enhancing mass in the renal sinus surrounding the neck of the middle calyx (arrows in **a** and **b**) with a filling defect in the calyceal neck in the excretory phase (arrow in **c**) and a calyceal

amputation in the CT urogram (arrow in **d**). On MRI the dilated calyx shows bleeding (arrow in **e**) and suspicious findings on diffusion-weighted imaging (arrow in **f**) with a clearly detectable enhancing mass along the calyceal neck (arrows in **g** and **h**)

the interstitium, with the nephrons, collecting ducts and blood vessels serving as a framework for tumour expansion, which produces the following patterns [45]:

- multiple poorly enhancing masses (60%)
- retroperitoneal tumours directly invading the kidneys (25–30%)
- infiltrative pattern with bilateral renal enlargement without disruption of the renal contour and perirenal soft-tissue masses

Fig. 7 CT imaging presentation (courtesy of Siegfried Schwab, University Hospital Erlangen, Germany; with permission) of renal lymphoma with unilateral (arrows in **a–c**) and bilateral (arrows in **d**) hypoenhancing focal masses with diffuse renal swelling and perirenal oedema. Small masses can be found in the cortex and with signs of infiltration of the perirenal space (arrow in **c**)



- cystic lesions and tumours predominantly affecting the renal sinus and collecting system are uncommon

Image-guided percutaneous biopsy is essential for diagnostic confirmation to avoid unnecessary nephrectomy. Following treatment, imaging findings may resolve with minimal residual scarring [32].

CT Contrast-enhanced CT remains the technique of choice for the detection, diagnosis, staging and monitoring of renal lymphoma [46, 47].

MRI Besides the morphological patterns already mentioned, lymphomatous masses are, relative to the renal cortex, iso- or slightly hypointense on T1-weighted images and hypointense on T2-weighted images. Minimal heterogeneous enhancement is seen on early and delayed gadolinium-enhanced MR images in retroperitoneal masses and renal involvement [32, 48].

6. Angiomyolipoma

Angiomyolipomas (Fig. 8) are hamartomas containing varying proportions of fat, smooth muscle and thick-walled blood vessels. Tumours larger than 4 cm carry an increased risk of potentially life-threatening haemorrhage (Wunderlich syndrome), which has been reported in up to 10% of these patients [32].

CT Lipid-containing angiomyolipoma can be easily detected with CT.

However, angiomyolipoma may contain very small quantities of fat, which can be overlooked if the mass is not carefully evaluated. When a small amount of fat is suspected in a renal mass, an unenhanced CT examination with thin sections and, if necessary, a pixel analysis, is the most sensitive test [31, 49].

Lipid-poor angiomyolipoma presents a diagnostic dilemma and cannot be differentiated from RCC. Zhang et al.

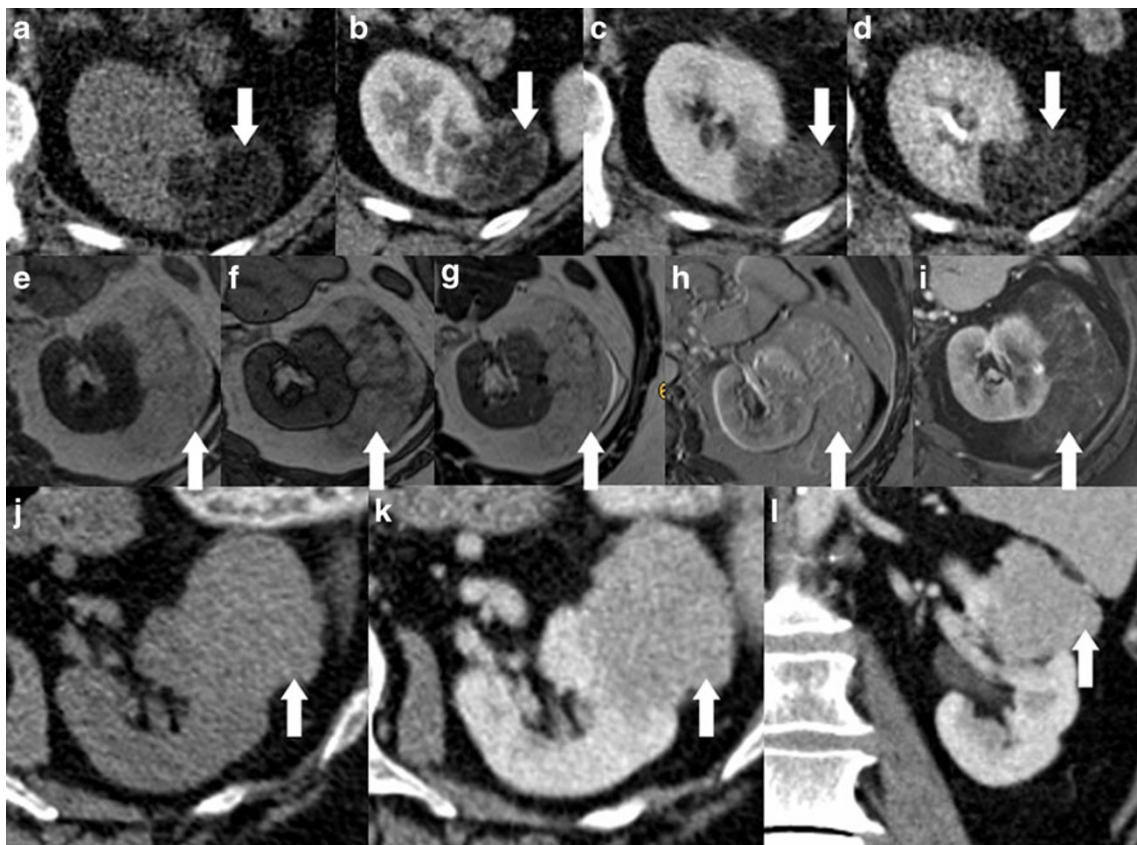


Fig. 8 Imaging presentation of angiomyolipoma (AML) in CT (upper and lower row) and MRI (middle row). On CT (upper row) lipid-containing AML shows bulk fat in the native (arrow in **a**) and moderate enhancement in the arterial (arrow in **b**), venous (arrow in **c**) and excretory phase (arrow in **d**). On MRI (middle row) another lipid-containing AML shows streaky signal alteration on in- and opposed-

phase T1-weighted imaging (arrows in **e** and **f**), heterogeneous pattern with high signal intensity on T2 T2 (arrow in **g**), a moderate enhancement on T1 (arrow in **h**), and a clear signal loss on the T1-weighted image with fat saturation (arrow in **i**). On CT (lower row) a lipid-poor AML is not clearly distinguishable from other renal masses in the native (arrow in **i**) and venous phase (arrows in **j** and **k**)

described a homogeneous pattern and a moderate enhancement of lipid-poor angiomyolipomas [13].

MRI Lipid-containing angiomyolipomas show a higher signal intensity than renal parenchyma on T1-weighted images. Demonstration of bulk fat within an angiomyolipoma can be achieved by applying a selective fat-suppression pulse. Opposed-phase imaging shows a characteristic India ink artifact at the interface between the mass and the normal renal parenchyma. The signal loss can be helpful for the diagnosis of lipid-poor angiomyolipomas, but clear cell RCC can also show small amounts of intracellular fat. The presence of central necrosis suggests the diagnosis of RCC, a finding that is very rare in angiomyolipoma. Lipid-poor angiomyolipomas frequently demonstrate homogeneous low signal intensity relative to the renal parenchyma on T2-weighted images. Angiomyolipomas can show different degrees of enhancement depending on the amount of vascularised tissue components they contain [32, 50, 51].

However, all the mentioned imaging characteristics are not specific enough to make a confident diagnosis of a non-fat-containing angiomyolipoma. In some cases, biopsy of the renal mass may be indicated to make a definitive diagnosis of an angiomyolipoma and to avoid surgery [31].

7. Oncocytoma

Oncocytomas (Fig. 9) account for 3–7% of solid renal masses. They may be multicentric, bilateral or metachronous in a minority of cases. A stellate central area of

fibrosis or hyalinised connective tissue with compressed blood vessels, the so-called central scar, is observed in up to 54% of cases. Based on imaging findings a proper differentiation between oncocytoma and RCC is not possible [32].

CT Oncocytoma remains a diagnostic challenge. Zhang et al. found that oncocytoma tended to show a homogeneous and hypervascular pattern. A central scar can be seen in large oncocytoma [13].

MRI Appearance is variable and non-specific. Oncocytomas are typically spheric and well-defined masses. Relative to the renal cortex, they have lower signal intensity on T1-weighted images in approximately 70% and higher signal intensity on T2-weighted images in up to 67%. The central scar (when present) can be seen as a stellate area of high signal intensity on T2-weighted images and of low signal intensity on T1-weighted images with delayed gadolinium enhancement. A well-defined hypointense capsule can be seen surrounding the tumour in almost one-half of renal oncocytomas. However, the presence of a pseudocapsule is non-specific and can be seen in up to 60% of RCCs as well [32, 52].

8. Pyelonephritis/abscess/xanthogranulomatous pyelonephritis/renal infarction

Bacterial pyelonephritis (PN) usually is an ascending infection from the lower urinary tract and can affect one or both kidneys. Haematogenous spread of bacteria is rare and usually affects both kidneys.

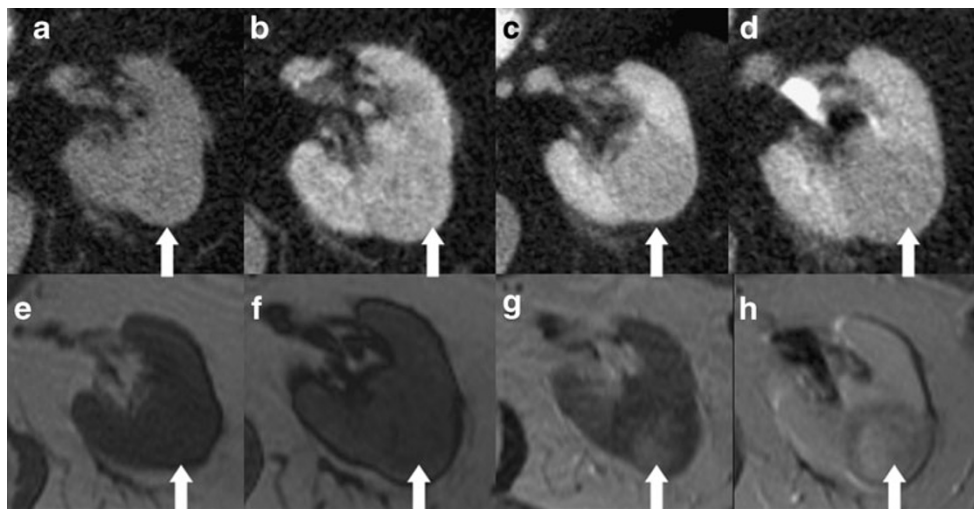


Fig. 9 Imaging presentation of adenoma on CT (upper row) and MRI (lower row) in one patient. CT shows a native isodense mass (arrow in a) with a hyperenhancement in the arterial phase (arrow in b), and an early wash-out in the venous (arrow in c) and excretory (arrow in d) phases. MRI shows a non-lipid-containing mass on the in- and

opposed-phase T1-weighted imaging (arrows in e and f) with a heterogeneous appearance in T2- (arrow in g) and a heterogeneous contrast media enhancement in T1-weighted image (arrow in h). Based on imaging features alone, this mass cannot be differentiated from RCC

Xanthogranulomatous pyelonephritis (XP) (Fig. 10) results from severe chronic infection causing diffuse renal destruction. Risk factors include female gender and diabetes. Most patients have nephrolithiasis, and staghorn calculi are found in 50% of patients. The more common diffuse form is characterised by extensive involvement of the renal parenchyma. The focal form of the disease may be misinterpreted as a renal neoplasm; the presence of a staghorn calculus, appropriate clinical presentation and the characteristic imaging findings strongly suggest the diagnosis [32]. CT is helpful in the detection of calculi.

CT In the case of PN unenhanced CT may appear normal, but acute bacterial nephritis most commonly manifests as one or more wedge-shaped areas or streaky zones of lesser enhancement that extend from the papilla to the renal cortex. Abscesses can be identified in CT as round or geographic low-attenuation collections with no central enhancement, but an enhancing rim (pseudo-capsules with wall thicknesses and frequent nodularity). Diminished

enhancement may surround the abscess (halo sign) during the nephrographic phase. Extraparenchymal collections can extend into adjacent structures (e.g., psoas muscle).

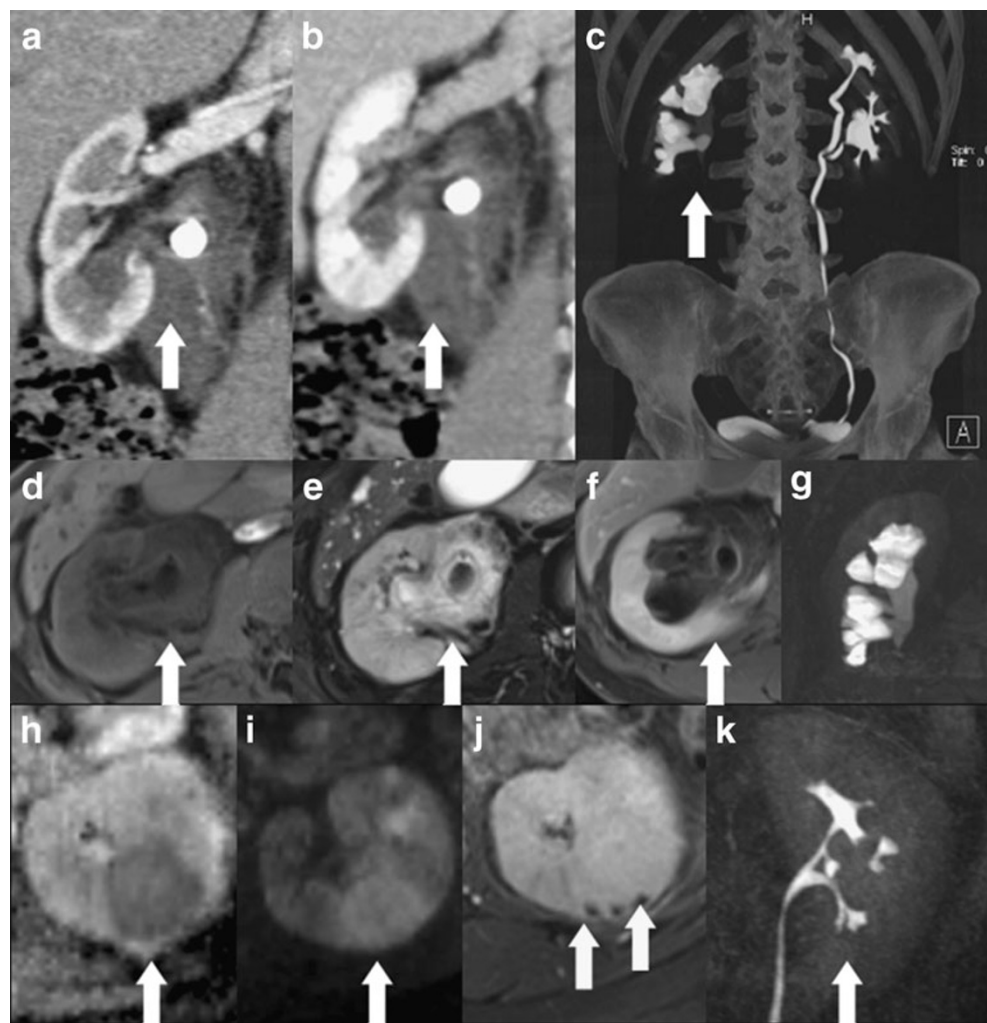
MRI The value of MR imaging for early diagnosis of pyelonephritis is still under debate.

Heterogeneous enhancement of renal tissue can also be seen with MR imaging. Probably DWI is helpful because of its high sensitivity in the detection of parenchymal oedema.

Magnetic resonance imaging findings of abscesses are similar to those of CT and include renal oedema, haemorrhage, renal enlargement, abscesses and perinephric fluid [53]. Abscess cavities show intermediate signal on T1-weighted images and high signal intensity on T2-weighted images. Cavity walls may show marked gadolinium enhancement. Calculi may be seen as areas of signal void within the collecting system [32, 54].

Renal infarction (RI) can have various causes, including thromboembolism, renal artery thrombosis, vasculitis, shock and trauma.

Fig. 10 Imaging presentation of xanthogranulomatous pyelonephritis (XP) and bacterial pyelonephritis (PN) on CT and MRI: XP on CT (upper row): a pelvic stone is clearly visible with a diffuse thickening of the pelvic wall, which shows enhancement in the arterial (arrow in **a**) and venous (arrow in **b**) phase. The CT urogram (arrow in **c**) shows the hydronephrosis owing to an obstruction at the level of the ureteropelvic junction. XP on MRI (middle row): the thickening of the pelvic wall is clearly detectable on T1-weighted (arrow in **d**) and T2-weighted (arrow in **e**) images, and an enhancement of the pelvic wall in T1 in the venous (arrow in **f**) phase. Contrast-enhanced MRI urogram (**g**) enables a similar presentation of the upper urinary tract in comparison to the CT urogram. PN on MRI (lower row): ADC mapping shows a decreased signal (arrow in **h**) and DWI (b-value: 800) a heterogeneous pattern of renal parenchyma (arrow in **i**). In the venous phase small non-enhanced subcapsular areas are detectable (arrow in **j**). MR urogram shows no hydronephrosis in this case of ascending PN (arrow in **k**)



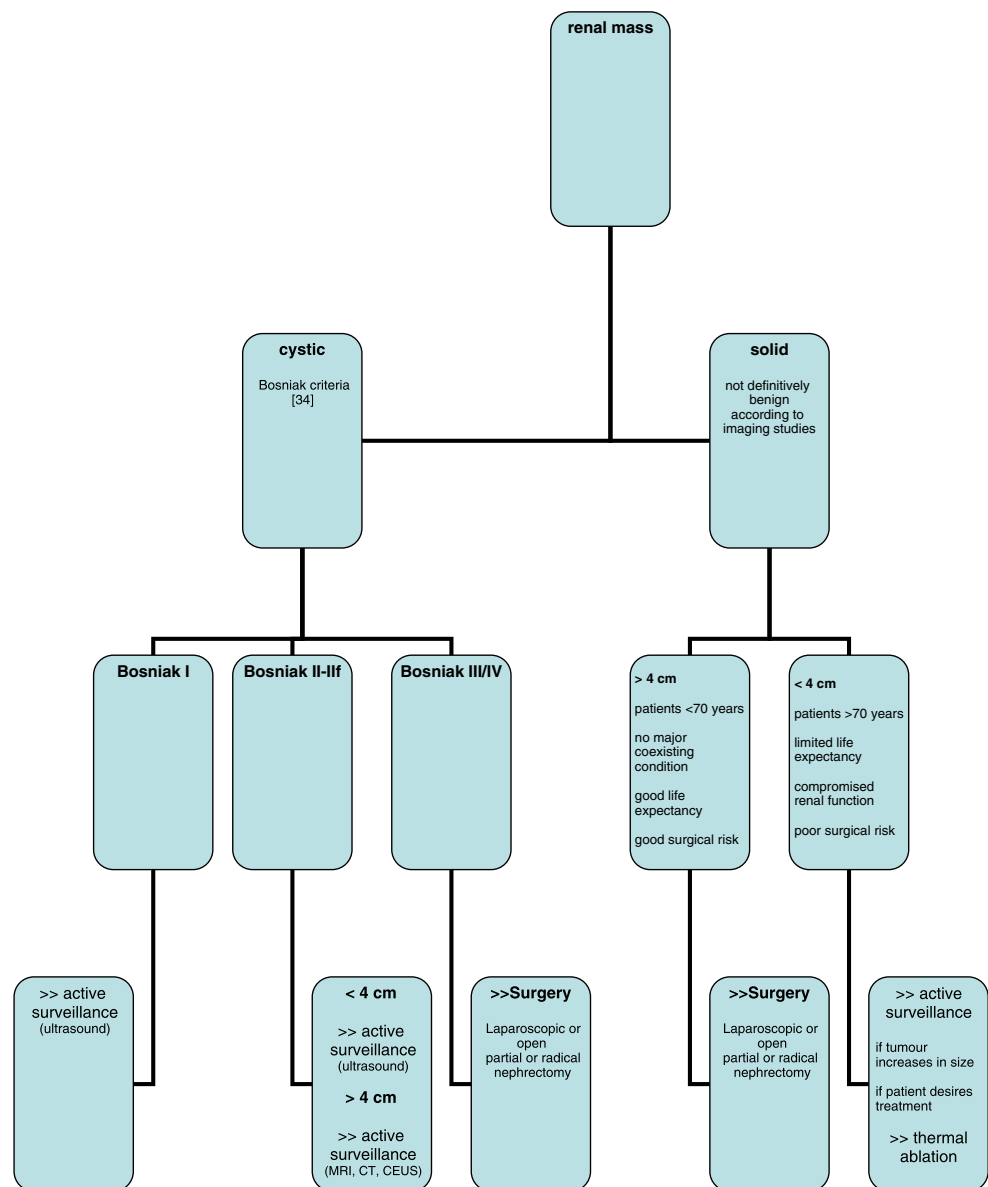
CT CT shows a swelling of the kidney, usually with perirenal fluid. Other findings are subcapsular haematoma, mass effect or a focal area of renal enlargement, and a thickened renal fascia. On post-contrast images a demarcation of the wedge-shaped infarcted areas is possible. The ischaemic areas are mainly located in the columns of the kidney contrary to inflammatory alterations, which can be located in the renal pyramids in the case of ascending infection.

MRI On T1- and T2-weighted MR images, the signal intensity of the infarcted area is usually lower than that of the non-infarcted area owing to interstitial oedema and haemorrhage, with a loss of corticomedullary differentiation. In the follow-up signal intensity increases progressively with both sequences because of coagulation necrosis

and interstitial haemorrhage. Post-contrast T1-weighted images clearly demonstrate wedge-shaped infarcted areas. The non-infarcted portion of the involved kidney may have higher signal intensity than the opposite uninvolved kidney on T2-weighted images and post-contrast T1-weighted images because of acute tubular necrosis and interstitial oedema at the margin of the infarct or reperfusion injury. With development of cortical atrophy and organising fibrosis (after weeks) the signal intensity of the infarcted area decreases again. The extent and distribution of the infarcted areas at MR imaging correlate well with CT and angiography [55].

VI. Clinical management/role of percutaneous renal mass biopsy

Fig. 11 Clinical flow chart of renal masses (modified according to Gill et al. [19])



Imaging can help to support clinical management in patients with renal masses by depicting certain lesions that do not require treatment. MRI and CT are useful for follow-up, and helpful for planning specific surgical approaches. In unclear solid lesions a percutaneous renal mass biopsy (RMB) has to be considered. The use of RMB has increased in recent years, despite concerns about safety, accuracy and sampling errors [19]. New biopsy techniques decrease the risk of tumour seeding, and overall morbidity is low. Diagnostic sufficiency and accuracy of RMB are now much higher in large-volume, experienced centres [56, 57]. Experienced users can achieve accurate diagnosis in over 90%. Pretreatment RMB can significantly decrease the number of unnecessary surgeries for benign disease and assist in clinical decision-making, beyond documenting renal involvement for patients with metastatic disease or other systemic illnesses. Especially for elderly and unfit patients who are possible candidates for active surveillance and/or minimally invasive ablative therapies, RMB seems to be a valuable tool. Finally, there is the potential for stratifying the initial therapy of metastatic RCC by histological subtype on needle biopsies [58]. Another study group concluded that percutaneous renal needle core biopsy has an acceptable sensitivity and specificity in the diagnosis of renal masses. The major limitation of percutaneous core biopsy is the technical failure that leads to insufficient material for accurate diagnosis [56, 57].

Furthermore, diagnostic and therapeutic decisions depend on the age and condition of the patient (see Fig. 11).

Conclusion

The technical developments in CT and MRI in the last decade enable an excellent detection rate of renal masses. Contrast-enhanced images allow differentiation between cystic and solid renal lesions. Complex cystic and solid lesions can be characterised further. Pretreatment percutaneous biopsy can significantly decrease the number of unnecessary surgeries for benign disease and assist the urologist in clinical decision-making, especially for elderly and unfit patients who are possible candidates for active surveillance and/or minimally invasive ablative therapies.

Acknowledgement Special thanks to Siegfried Schwab from the University Hospital Erlangen, Germany, for providing us with CT cases of renal lymphoma.

References

1. Srougi V, Kato RB, Salvatore FA, Ayres PP, Dall'Oglio MF, Srougi M (2009) Incidence of benign lesions according to tumor size in solid renal masses. *Int Braz J Urol* 35(4):427–431
2. Coulam CH, Sheafor DH, Leder RA, Paulson EK, DeLong DM, Nelson RC (2000) Evaluation of pseudoenhancement of renal cysts during contrast-enhanced CT. *AJR Am J Roentgenol* 174(2):493–498
3. Tada S, Yamagishi J, Kobayashi H, Hata Y, Kobari T (1983) The incidence of simple renal cyst by computed tomography. *Clin Radiol* 34:437–439
4. Pahernik S, Ziegler S, Roos F, Melchior SW, Thüroff JW (2007) Small renal tumors: correlation of clinical and pathological features with tumor size. *J Urol* 178:414–417, discussion 416–417
5. Jemal A, Siegel R, Ward E, Hao Y, Xu J, Murray T et al (2008) Cancer statistics, 2008. *CA Cancer J Clin* 58:71–96
6. Chow WH, Devesa SS, Warren JL, Fraumeni JF Jr (1999) Rising incidence of renal cell cancer in the United States. *JAMA* 281:1628–1631
7. D'Antonio A, Caleo A, Caleo O, Adesso M, Boscaio A (2010) Hepatocellular carcinoma metastatic to the kidney mimicking renal oncocytoma. *Hepatobiliary Pancreat Dis Int* 9(5):550–552
8. Kovacs G, Akhtar M, Beckwith BJ et al (1997) The Heidelberg classification of renal cell tumours. *J Pathol* 183:131–133
9. Motzer RJ, Bacik J, Mariani T, Russo P, Mazumdar M, Reuter V (2002) Treatment outcome and survival associated with metastatic renal cell carcinoma of non-clear-cell histology. *J Clin Oncol* 20:2376–2381
10. Choh NA, Jehangir M, Choh SA (2010) Renal replacement lipomatosis: a rare type of renal pseudotumor. *Indian J Nephrol* 20(2):92–93
11. Tarhan F, Gül AE, Karadayi N, Kuyumcuoğlu U (2004) Inflammatory pseudotumor of the kidney: a case report. *Int Urol Nephrol* 36(2):137–140
12. Joffe SA, Servaes S, Okon S, Horowitz M (2003) Multi-detector row CT urography in the evaluation of hematuria. *Radiographics* 23(6):1441–1455
13. Zhang J, Pedrosa I, Rofsky NM (2003) MR techniques for renal imaging. *Radiol Clin North Am* 41:877–907
14. Silverman SG, Leyendecker JR, Amis ES Jr (2009) What is the current role of CT urography and MR urography in the evaluation of the urinary tract? *Radiology* 250(2):309–323
15. Nikken JJ, Krestin GP (2007) MRI of the kidney – state of the art. *Eur Radiol* 17:2780–2793, Review
16. Al-Okaili RN, Krejza J, Wang S, Woo JH, Melhem ER (2006) Advanced MR imaging techniques in the diagnosis of intra-axial brain tumors in adults. *Radiographics* 26(Suppl 1):S173–S189
17. Zhang J, Tehrani YM, Wang L, Ishill NM, Schwartz LH, Hricak H (2008) Renal masses: characterization with diffusion-weighted MR imaging—a preliminary experience. *Radiology* 247(2):458–464
18. Sandrasegaran K, Sundaram CP, Ramaswamy R, Akisik FM, Rydberg MP, Lin C, Aisen AM (2010) Usefulness of diffusion-weighted imaging in the evaluation of renal masses. *AJR Am J Roentgenol* 194(2):438–445
19. Gill IS, Aron M, Gervais DA, Jewett MAS (2010) Small renal mass. *N Engl J Med* 362:624–634
20. Kreft BP, Müller-Miny H, Sommer T, Steudel A, Vahlensieck M, Novak D, Müller BG, Schild HH (1997) Diagnostic value of MR imaging in comparison to CT in the detection and differential diagnosis of renal masses: ROC analysis. *Eur Radiol* 7(4):542–547
21. Frank I, Blute ML, Chevillie JC, Lohse CM, Weaver AL, Zincke H (2003) Solid renal tumors: an analysis of pathological features related to tumor size. *J Urol* 170:2217–2220
22. Chawla SN, Crispin PL, Hanlon AL, Greenberg RE, Chen DY, Uzzo RG (2006) The natural history of observed enhancing renal masses: meta-analysis and review of the world literature. *J Urol* 175:425–431

23. Klatte T, Patard JJ, de Martino M et al (2008) Tumor size does not predict risk of metastatic disease or prognosis of small renal cell carcinomas. *J Urol* 179:1719–1726
24. Remzi M, Ozsoy M, Klingler HC et al (2006) Are small renal tumors harmless? Analysis of histopathological features according to tumors 4 cm or less in diameter. *J Urol* 176:896–899
25. Schurich M, Pallwein L, Steiner H, Mallouhi A, zur Nedden D, Frauscher F (2005) The role of Multiphasic Helical CT in estimation of type of renal cell carcinoma: an approach based on standardized morphological and enhancement parameters (abstract for poster presentation LPH06-04) In: Radiological Society of North America scientific assembly and annual meeting program. Oak Brook, IL. Available at http://rsna2005.rsna.org/rsna2005/V2005/conference/event_display.cfm?em_id=4419040
26. Siu W, Hafez KS, Johnston WK III, Wolf JS Jr (2007) Growth rates of renal cell carcinoma and oncocytoma under surveillance are similar. *Urol Oncol* 25:115–119
27. Kunkle DA, Crispen PL, Chen DYT, Greenberg RE, Uzzo RG (2007) Enhancing renal masses with zero net growth during active surveillance. *J Urol* 177:849–854
28. Silverman SG, Israel GM, Herts BR, Richie JP (2008) Management of the incidental renal mass. *Radiology* 249:16–31
29. Kim JK, Kim SH, Jang YJ et al (2008) Renal angiomyolipoma with minimal fat: differentiation from other neoplasms at double-echo chemical shift FLASH MR imaging. *Radiology* 239:174–180
30. Israel GM, Bosniak MA (2008) Pitfalls in renal mass evaluation and how to avoid them. *Radiographics* 28(5):1325–1338, Review
31. Outwater EK, Bhatia M, Siegelman ES, Burke MA, Mitchell DG (1997) Lipid in renal clear cell carcinoma: detection on opposed-phase gradient-echo MR images. *Radiology* 205:103–107
32. Pedrosa I, Sun MR, Spencer M, Genega EM, Olumi AF, Dewolf WC, Rofsky NM (2008) MR imaging of renal masses: correlation with findings at surgery and pathologic analysis. *Radiographics* 28:985–1003
33. Wagner BJ (1997) The kidney: radiologic-pathologic correlation. *Magn Reson Imaging Clin N Am* 5:13–28
34. Israel GM, Hindman N, Bosniak MA (2004) Evaluation of cystic renal masses: comparison of CT and MR imaging by using the Bosniak classification system. *Radiology* 231(2):365–371
35. Koga S, Nishikido M, Inuzuka S, Sakamoto I, Hayashi T, Hayashi K, Saito Y, Kanetake H (2000) An evaluation of Bosniak's radiological classification of cystic renal masses. *BJU Int* 86(6):607–609
36. Xu HX (2009) Contrast-enhanced ultrasound: the evolving applications. *World J Radiol* 31(1):15–24
37. Novara G, Martignoni G, Artibani W, Ficarra V (2007) Grading systems in renal cell carcinoma. *J Urol* 177:430–436
38. Chevillat JC, Lohse CM, Zincke H, Weaver AL, Blute ML (2003) Comparisons of outcome and prognostic features among histologic subtypes of renal cell carcinoma. *Am J Surg Pathol* 27:612–624
39. Ruppert-Kohlmayr AJ, Uggowitz M, Meissnitzer T, Ruppert G (2004) Differentiation of renal clear cell carcinoma and renal papillary carcinoma using quantitative CT enhancement parameters. *AJR Am J Roentgenol* 183:1387–1391
40. Roy C, Sauer B, Lindner V, Lang H, Saussine C, Jacqmin D (2007) MR imaging of papillary renal neoplasms: potential application for characterization of small renal masses. *Eur Radiol* 17:193–200
41. Yoshimitsu K, Kakihara D, Irie H et al (2006) Papillary renal carcinoma: diagnostic approach by chemical shift gradient-echo and echo-planar MR imaging. *J Magn Reson Imaging* 23:339–344
42. Vikram R, Sandler CM, Ng CS (2009) Imaging and staging of transitional cell carcinoma: part 2, upper urinary tract. *AJR Am J Roentgenol* 192(6):1488–14893, Review
43. Pickhardt PJ, Lonergan GJ, Davis CJ Jr, Kashitani N, Wagner BJ (2000) From the archives of the AFIP: infiltrative renal lesions—radiologic-pathologic correlation. *Radiographics* 20:215–243
44. Hulnick DH, Bosniak MA (1986) “Faceless kidney”: CT sign of renal duplicity. *J Comput Assist Tomogr* 10:771–772
45. Sheth S, Ali S, Fishman E (2006) Imaging of renal lymphoma: patterns of disease with pathologic correlation. *Radiographics* 26(4):1151–1168, Review
46. Urban BA, Fishman EK (2000) Renal lymphoma: CT patterns with emphasis on helical CT. *Radiographics* 20:197–212
47. Semelka RC, Kelekis NL, Burdeny DA, Mitchell DG, Brown JJ, Siegelman ES (1996) Renal lymphoma: demonstration by MR imaging. *AJR Am J Roentgenol* 166:823–827
48. Pinggera GM, Peschel R, Buttazzoni A, Mitterberger M, Friedrich A, Pallwein L (2009) A possible case of primary renal lymphoma: a case report. *Cases J* 2:6233
49. Simpfendorfer C, Herts BR, Motta-Ramirez GA, Lockwood DS, Zhou M, Leiber M, Remer EM (2009) Angiomyolipoma with minimal fat on MDCT: can counts of negative-attenuation pixels aid diagnosis? *AJR Am J Roentgenol* 192(2):438–443
50. Israel GM, Hindman N, Hecht E, Krinsky G (2005) The use of opposed-phase chemical shift MRI in the diagnosis of renal angiomyolipomas. *AJR Am J Roentgenol* 184:1868–1872
51. Burdeny DA, Semelka RC, Kelekis NL, Reinhold C, Ascher SM (1997) Small (<1.5 cm) angiomyolipomas of the kidney: characterization by the combined use of in-phase and fat-attenuated MR techniques. *Magn Reson Imaging* 15:141–145
52. Harmon WJ, King BF, Lieber MM (1996) Renal oncocytoma: magnetic resonance imaging characteristics. *J Urol* 155:863–867
53. Verswijvel G, Oyen R, Van Poppel H, Roskams T (2000) Xanthogranulomatous pyelonephritis: MRI findings in the diffuse and the focal type. *Eur Radiol* 10:586–589
54. Craig WD, Wagner BJ, Travis MD (2008) Pyelonephritis: radiologic-pathologic review. *Radiographics* 28(1):255–277, quiz 327–328. Review
55. Jeong JY, Kim SH, Lee HJ, Sim JS (2002) Atypical low-signal-intensity renal parenchyma: causes and patterns. *Radiographics* 22(4):833–846, Review
56. Wang R, Li AY, Wood DP Jr (2011) The role of percutaneous renal biopsy in the management of small renal masses. *Curr Urol Rep* 12(1):18–23
57. Sofikerim M, Tatlisin A, Canoz O, Tokat F, Demirtas A, Mavili E (2010) What is the role of percutaneous needle core biopsy in diagnosis of renal masses? *Urology* 76(3):614–618
58. Volpe A, Terrone C, Scarpa RM (2009) The current role of percutaneous needle biopsies of renal tumours. *Arch Ital Urol Androl* 81(2):107–112, Review